Synthesis, Characterization, Crystal Structure, Hirshfeld surface analysis and DFT studies of novel compounds based on the methoxynaphthalene ring

El-Mahdi Ourhzif, Isabelle Abrunhosa-Thomas, Pierre Chalard, Mostafa Khouili, Yves Troin, Mohamed Akssira, El Mostafa Ketatni

▶ **To cite this version:**

El-Mahdi Ourhzif, Isabelle Abrunhosa-Thomas, Pierre Chalard, Mostafa Khouili, Yves Troin, et al.. Synthesis, Characterization, Crystal Structure, Hirshfeld surface analysis and DFT studies of novel compounds based on the methoxynaphthalene ring. Journal of Molecular Structure, 2021, 1244, pp.130947. 10.1016/j.molstruc.2021.130947 . hal-03468258

HAL Id: hal-03468258
https://uca.hal.science/hal-03468258v1

Submitted on 13 Jun 2023

HAL is a multi-disciplinary open access archive for the deposit and dissemination of scientific research documents, whether they are published or not. The documents may come from teaching and research institutions in France or abroad, or from public or private research centers.

L'archive ouverte pluridisciplinaire **HAL**, est destinée au dépôt et à la diffusion de documents scientifiques de niveau recherche, publiés ou non, émanant des établissements d'enseignement et de recherche français ou étrangers, des laboratoires publics ou privés.

Distributed under a Creative Commons Attribution - NonCommercial 4.0 International License

Version of Record: https://www.sciencedirect.com/science/article/pii/S002228602100644X
Manuscript_9fb35994b1a502ec29633224d4f32338

Crystal Structure, Hirshfeld surface analysis and DFT studies of *Euphorbioside* Monhydrate a Major Bisnorsesquiterpene Isolated from *Euphorbia resinifera* latex

El-Mahdi Ourhzif[a,b,c], El Mostafa Ketatni[a*], Mohamed Akssira[b], Yves Troin[c] and Mostafa Khouili[a*]

[a] Laboratory of Organic and Analytical Chemistry, Sultan Moulay Slimane University, Faculty of Science and Technology, BP 523, 23000 Beni-Mellal, Morocco
[b] Laboratoire de Chimie Physique et Chimie Bio-organique, URAC 22 Université Hassan II, Mohammedia-Casablanca, BP 146, 28800, Mohammedia, Morocco
[c] Université Clermont Auvergne, CNRS, SIGMA Clermont, ICCF, F-63000 Clermont-Ferrand, France

[*]*Correspondence e-mail: mostafakhouili@gmail.com, elm_ketatni@hotmail.fr,*

© 2021 published by Elsevier. This manuscript is made available under the CC BY NC user license
https://creativecommons.org/licenses/by-nc/4.0/

ABSTRACT:

The structure of this new derivative of *Euphorbioside* [systematic name: (1S,2R,3R,5R,8R)-8-((R,E)-3-hydroxybut-1-en-1-yl)-1,5-dimethyl-6-oxabicyclo[3.2.1]octane-2,3-diol hydrate] was determined by its single-crystal X-ray structure, and to studies with the use of NMR, LC/HRMS and IR spectra. The title compound is built up from two fused five- and six-membered rings, with an additional hydroxybut-1-en-1-yl group and water molecule. The five-membered ring, which has an envelope conformation, makes dihedral angles of 77.46(13)° with the benzene ring. The water molecule forms O—H…O hydrogen bond. In the crystal, intermolecular O—H…O and C—H…O hydrogen bonds lead to the formation of three-dimensional framework**.** The nature of intermolecular interactions in the supramolecular structure Hirshfeld surface analysis and 2D fingerprint was carried out. The most important contributions for the crystal packing are from H···H (75.2%) and O···H/H···O (24.6%) interactions. Additionally, DFT calculations have been used to analyze the electronic and geometric frontier molecular orbital, Molecular Electrostatic Potential map analyses, Mulliken and Natural bond charges were produced by using the optimized structures.

Keywords
Euphorbia, Euphorbioside, *Euphorbia resinifera* Berg, Crystal Structure, Hydrogen bond, Hirshfeld surface analysis, DFT, NBO

1. Introduction

Natural products have become a key source of new drugs in the last years [1,2]. The *Euphorbia* is the most important genus of the family Euphorbiaceae, with there being more than 2000 species in the world which are characterized by the presence of an irritant latex rich in triterpenes [3]. The largest species of the Euphorbiaceae family, have been studies due to the presence of numerous bioactive terpenoids, diterpenoids, triterpenes, sesquiterpenoids and other constituents in *Euphorbia* [4-8]. *Euphorbia resinifera* Berg., is a Moroccan endemic plant, where it occurs on the slopes of the anti-Atlas Mountains of Morocco [9]. *E. resinifera.* Berg., belongs to the *Euphorbia*, one of the most important medicinal families of plants. The medicinal use of Euphorbium, is the dried latex of *Euphorbia resinifera*, reflects a history more than 2000 years old, which makes resiniferatoxin (RTX) one of the most ancient drugs still in which is being used as a starting point in the development of a novel class of analgesics [10-12]. Furthermore, Euphorbium is used in Moroccan traditional medicine to suppress chronic pain, dental cavities to mitigate tooth ache, tuberculosis [13].

The title compound, $C_{13}H_{22}O_4.H_2O$, {systematic name: (1S,2R,3R,5R,8R)-8-((R,E)-3-hydroxybut-1-en-1-yl)-1,5-dimethyl-6-oxabicyclo[3.2.1]octane-2,3-diol hydrate, is a bisnorsesquiterpene of the dihydroionol type which was isolated from the dried latex of *Euphorbia resinifera* Berg. The structure of title compound was established by ^{1}H and ^{13}C NMR spectra, LC/HRMS, IR spectra and confirmed by its single-Crystal X-ray structure. Additionally, we have enriched the work by theoretical calculations with investigation HOMO-LUMO energies, Molecular electrostatic potential surface map, natural bond analysis (NBO) and analysis of Hirshfeld surface.

2. Experimental

2.1. General experimental

Thin-layer chromatography **(TLC)** were performed on pre-coated silica plates Kiesilgel 60F254 (Merck) or glass backed silica Duracil 25 UV254 (Macherey-Nagel). Spots were visualized using short (254 nm) UV light before using an ethanolic solution of phosphomolybdic acid (heating). Purifications by column chromatography were performed using silica gel Kiesgel 60, 40–63 µm. Melting points **(mp)** were measured by a Kofler hot bench or Reichert plate-heating microscope and are reported uncorrected. **IR** spectra were obtained using IRAffinity-1S FTIR Infrared spectrophotometer. Measurements were made by loading the sample directly onto a diamond cell. The measurements are reported on the

wavenumber scale (cm–1). ^{1}H and ^{13}C **NMR** spectra were recorded on a Brüker Avance spectrometer at 400.13 and 100.61 MHz respectively using CD_3OD-*d4* as solvent. Chemical shifts (^{1}H and ^{13}C) were reported in ppm relative to solvent residual signals, (CD_3OD-*d4*: δ ^{1}H = 4.87 ppm and δ ^{13}C = 49.00 ppm. Spectra were processed with Mnova program from MestRelab Research. Coupling constants *J* were given in Hertz (Hz). The abbreviations used for signal descriptions are as: s (singlet), d (doublet), dd (doublet of doublets), ddd (doublet of doublets of doublets), q (quartet). **LC–HRMS** was recorded a Q Exactive Quadrupole-Orbitrap mass spectrometer coupled to a HPLC Ultimate 3000 (Kinetex EVO C18; 1.7 μm; 100 mm × 2.1 mm column with a flow rate of 0.45 mL min−1 with the following gradient: a linear gradient of solvent B from 5% to 95% over 7.5 min (solvent A = H_2O + 0.1% formic acid, solvent B = acetonitrile + 0.1% formic acid) equipped with a DAD UV/vis 3000 RS detector. **X-ray** data were collected at 100 K with an Oxford Diffraction Xcalibur 2 diffractometer equipped with a copper microsource (λ = 1.5418 Å).

Plant Material

Latex from *Euphorbia resinifera* Berg, was collected in October, 2016, from plants on the area of Azilal, Morocco. Latex was obtained by making repeated cuts along the stems of the plants with a knife and collecting the white milky exudates. A voucher specimen (20161023) is on deposit at the herbarium of. Laboratory of Organic and Analytical Chemistry, Sultan Moulay Slimane University, Faculty of Science and Technology, BP 523, 23000 Beni-Mellal.

Extraction and Isolation

The latex (1.5 L) from *E. resinifera* Berg was allowed to dry and the resulting coagulum (600 g) was extracted with EtOH (2 L), employing a Sohxlet apparatus. After 24 h ethanolic extraxt was concentrated to obtain a crude gummy material (88.8 g). The concentrated extract was suspended in H_2O and successively partitioned with *n*-hexane, dichloromethane, ethyl acetate and *n*-butanol. The dried *n*-butanol fraction was then subjected to silica gel column chromatography, eluting with ethyl acetate increasing polarity with methanol, EtOAc/ MeOH (9 : 1 and 8 :2 (*v*/*v*)) to yield 4 fractions: FB.1–4. Fraction FB3 (230 mg) was further purified by column Chromatography on silica gel eluted with EtOAc/MeOH (9:1) system, yielding the title compound as white solid (40 mg). Colorless block-shaped single crystals of the title compound suitable for *x*-ray structure determination were recrystallized from ethyl acetate/MeOH by the slow evaporation of the solvent at room temperature after several days.

mp: 94-95 °C. IR ν_{max} (cm^{-1}): 3408.22, 3259.70, 3180.62, 1139.93, 1055.06, 987.55, 802.39. ^{1}H NMR and ^{13}C NMR (CD_3OD) spectral data see Table 1. LC/HRMS (ESI) m/z: calcd for $C_{13}H_{22}O_4$ [M+H-H_2O] 225.1485; found 225.1481, t_R= 2.30 min.

2.3. Crystal X-ray data collection

Reflection intensities for the title compound was measured on Bruker APEX-II CCD diffractometer and MoK_α graphite-monochromated radiation (= 0.71073 Å). SAINT$^+$ 6.02 program was used for extraction and integration of diffraction intensities and SADABS program was carried out for correction of absorption effect [14]. The structures were solved by direct methods using SHELXTL-2014/5 [15] and refined (by weighted full matrix least-square on F^2 technics) to convergence using the SHELXL-2018/3 program [16]. All non-hydrogen atoms were refined anisotropically. All hydrogen atoms were fixed geometrically and were allowed refined using a riding model. The C-bound H atoms were geometrically placed (C—H = 0.93–0.99 Å) and refined as riding with U_{iso}(H) = 1.2–1.5U_{eq}(C). The O-bound H-atom was located in a difference Fourier map and refined freely. The reflection (001), (-1 0 1) and (1 0 0) affected by the beam-stop, were removed during refinement.
Crystal data, data collection and structure refinement details are summarized in Table 2. Details on the crystallographic studies, as well as atomic displacement parameters, are given as Supporting Information in the form of cif files. The plot of the molecule and the three-dimensional drawing of the crystal structure are obtained using the Diamond programs [17].

2.4. Hirshfeld surface and 2D fingerprint plots.

The Hirshfeld surfaces calculated for $C_{13}H_{22}O_4.H_2O$ compound provide additional information on the distinctive contributions made to the molecular packing. Thus, a Hirshfeld surface analysis [18] and the associated two-dimensional fingerprint plots [19] were performed using CrystalExplorer17.5 [20] to figure out the normalized contact distance (d_{norm}), which depends on contact distances to the closest atoms outside (d_e) and inside (d_i) the surface. The molecular HS were performed using a standard (high) surface resolution with the three-dimensional surfaces mapped over a fixed color scale of -0.8273 to 1.4443a.u.

2.5 Quantum chemical calculations

Gaussian 09 W program was utilized to obtain the molecular geometry optimization of $C_{13}H_{22}O_4.H_2O$ and GaussView molecular visualization software [21, 22]. The molecular of

Euphorbioside hydrate was optimized by DFT using the B3LYP method and HF in the gas phase with a 6-31g(d,p) basic set [23-25]. The NBO analysis [26] was carried out utilizing the optimized geometry at the DFT and HF level in order to understand inter and intra-molecular delocalization or hyperconjugation. Molecular Electrostatic Potential (MEP) map allows up to visualize variably charged regions of the title compound.

3. Results and discussion

3.1. Synthesis

Euphorbiosides and related compound are the first sesquiterpenoids isolated from *Euphorbia resinifera* Berg., and represent only the second case of occurrence of sesquiterpenoids in spurges [27]. Many of these substances exhibit biological activities that have been recently reported [28]. In order to isolate similaire compounds and as part of a program to access chemical diversity of Moroccan traditional medicines and ther biological effets, we have investigeted of extraction and identification of the major compounds from air-dried latex of *Euphorbia resinifera* Berg.

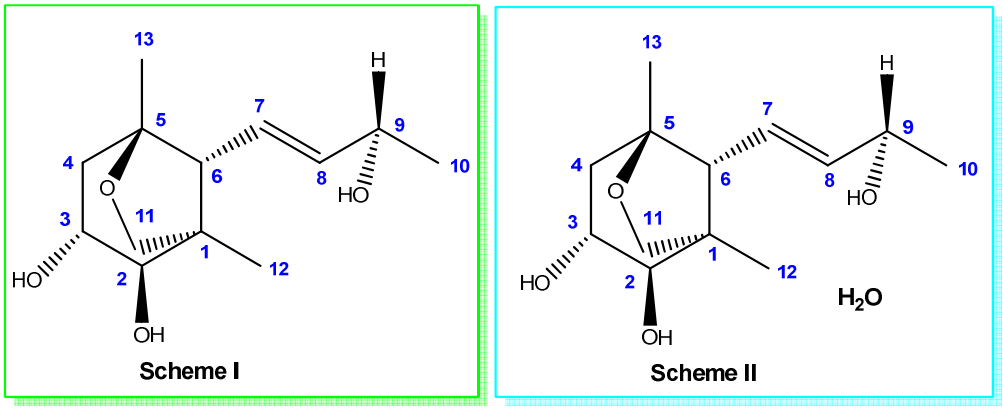

The structure of Euphorbioside C (Scheme I) previously elucidated by NMR spectroscopy in on study on bisnorsesquiterpenoids from *Euphorbia resinifera Berg* [9]. To the best of our knowledge, this is its first isolation from fresh latex of *Euphorbia resinifera* Berg. The isolated compound was identified by NMR spectra and the crystal structure of Euphorbioside C has not yet been reported. Herein we report the isolation and single-crystal X-ray diffraction studies of Euphorbioside monhydrate (scheme II).

Euphorbioside monohydrate was obtained as white crystals and had a molecular formula of $C_{13}H_{22}O4.H_2O$ based on LC/HRMS (ESI) calcd for ($C_{13}H_{22}O_4$ [M+H-H_2O] 225.1485; found 225.1481) and NMR data. The IR spectrum indicated the presence of hydroxyl (3408.22 cm^{-1}) group (Fig. SI1). The ^1H NMR spectrum (Table 1 and Fig. SI2) showed three methyl groups H_3-10, H_3-13 and H_3-12 [δ_H 1.29 (3H, d, 6.4), 1.18 (3H, s) and 1.04 (3H, s)], two olefinic

protons H-8 and H-7 [δ_H 5.80 (1H, dd, 15.3, 5.8) and 5.69 (1H, dd, 15.3, 9.6)], two methylene groups including an oxygen-bearing isolated methylene group H-4b and H-4a [δ_H 1.94 (1H, dd, 13.6, 6.5) and 1.63 (1H, dd, 13.6, 10.4), H-11b and H-11a [δ_H 4.02 (1H, d, 8.00) and 3.35 (1H, overlapped)], three oxymethine groups H-2, H-3 and H-9 [δ_H 3.55 (1H, d, 7.8), 3.74(1H, ddd, 10.4, 7.8, 6.5) and 4.32 (1H, q, 6.4)]. The ^{13}C NMR and ^{13}C APT (jmod) spectra (Fig. SI 3-4) displayed two quaternary carbons atoms, one of these oxygenated C-5 (δ_C 83.8), two methylene groups C-4 and C-11 (δ_C 42.9, 74.1), three methyl C-10, C-12, and C-13 (δ_C 24.5, 18.0 and 23.9) and six protonated carbon atoms including three oxygenated methin C-2, C-3, and C-9 (δ_C 76.6, 73.1 and 68.9) and two olefinic group C-7 and C-8 (δ_C 123.7 and 142.4). In addition, the coupling constant between H-7 and H-8, J =15.3 Hz, confirmed the *E* configuration at C-7/C-8. The resonances of protonated carbon atoms were associated with those of the directly attached hydrogen atoms through the 2D ^{1}H-detected HMQC experiment (Table 1 and Fig. SI5).

Table 1: ^{1}H NMR (400 MHz) and ^{13}C NMR (100 MHz) spectral data of Euphorbioside monohydrate (scheme I)

Position	type	δ_C (mult.)	δ_H (int., mult., J in Hz)
1	C	49.3	
2	CH	76.6	3.55 (1H, d, 7.8)
3	CH	73.1	3.74 (1H, ddd, 10.4, 7.8, 6.5)
4a	CH_2	42.9	1.63 (1H, dd, 13.6, 10.4)
4b			1.94 (1H, dd, 13.6, 6.5)
5	C	83.8	
6	CH	61.3	2.19 (1H, d, 6.9)
7	CH	123.7	5.69 (1H, dd, 15.3, 9.6)
8	CH	142.4	5.80 (1H, dd, 15.3, 5.8)
9	CH	68.9	4.32 (1H, q, 6.4)
10	CH_3	24.5	1.29 (3H, d, 6.4)
11a	CH_2	74.1	3.35[a]
11b			4.02 (1H, d, 8.0)
12	CH_3	18.0	1.04 (3H, s)
13	CH_3	23.9	1.18 (3H, s)

[a] Overlapping signals.

3.2. Crystal structure of the title compound

Euphorbioside-H_2O was crystallized from ethyl acetate/MeOH to give very white crystals suitable for single crystal X-ray measurements. The title compound crystallizes in the monoclinic system with non centrosymetric space group $P2_1$. The structural diagrams of the crystal structure determined in this study are shown in Scheme 1, and the crystallographic asymmetric-unit contents are shown in Fig. 1. The selected bond distances and angles are reported in Table 3. The compound is built up from two fused five- and six-membered rings with an additional hydroxybut-1-en-1-yl and water molecule. The configuration of the C7═C8 bond [1.318 (3)Å] of this Schiff base is *E*, stabilized by the intramolecular C7—H7...O3 hydrogen bond that forms an *S*(5) ring motif (Fig.1 and Table 4). In the molecule, there are six chiral C atoms: C1 exhibits an S configuration and C2, C3, C5, C6 and C9 exhibits an R configuration. The five-membered tetrahydrofuran (O2/C1/C5-C6/C11) ring, which has an envelope conformation on C6 atom, makes dihedral angles of 77.46(13)° with the benzene ring. The cyclohexane ring adopts a chair conformation, as indicated by the total puckering amplitude Q(T) = 0.637(2)Å and spherical polar angle θ = 21.92(18)° with φ= 300.2(6)°. In the cyclohexane diol, C—O_{Hy} bond length is 1.426 (3) Å while as started 1.434 Å in the previous reported structure [29, 30]. While the C—O bond in tetrahydrofuran is greater than those with hydroxyl group oxygen (C—O_{Hy}), in agreement with those found in bicyclic compounds in the literature (5-(3,8-dihydroxy-1,5-dimethyl-6-oxabicyclo[3.2.1]oct-8-yl)-3-methylpenta-2,4-dieonic acid hydrate [31].

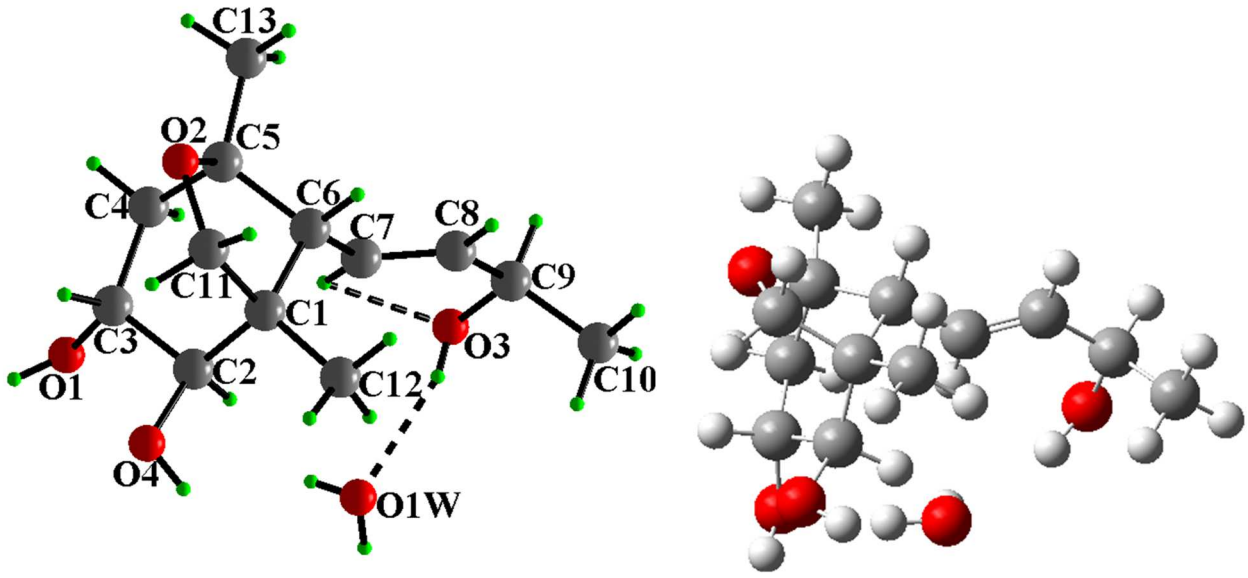

Figure 1 : The asymmetric unit of the title compound obtained from X-ray and DFT.

Table 2: Crystal Data, Summary of Intensity Data Collection, and Structure Refinement

Empirical formula	$C_{13}H_{22}O_4.H_2O$
Formula weight	260.32
Temperature (K)	293
Wavelength	0.71073 Å
Crystal system, space group	Monoclinic, $P2_1$
a, b, c (Å), β(°)	9.514 (6), 7.633 (6), 10.561 (6), 113.11 (2)
Volume (A^3)	705.4 (8)
Z	2
Calculated density (g/cm^3) (g/cm^3)	1.226
μ (mm^{-1})	0.09
Crystal shape and color	Plate, colorless
Crystal size (mm)	0.34x0.31x0.09
Theta range for data collection (°)	3.205– 31.132
Limiting indices	-15 ≤h ≤15, -29≤ k ≤29, -10 ≤ l≤ 10
Diffractometer	Bruker APEX-II CCD
Absorption correction	numerical (*SADABS*, Brucker, 2001)
Tmin. Tmax.	0.953, 0.986
No. of measured, independent and observed [$I > 2\sigma(I)$] reflections	21427, 3087, 2855 [R(int) = 0.031]
Refinement method	Full-matrix least-squares on F^2
Data / restraints / parameters	3087/1/185
R[$F^2 > 2\sigma(F^2)$], wR(F^2), S	0.034,0.093, 1.06
H-atom treatment	H atoms treated by a mixture of independent and constrained refinement
$\Delta\rho_{max}$, $\Delta\rho_{min}$ (e $Å^{-3}$)	0.43, –0.19

The water molecule connect three *Euphorbioside* via O1W—H1W…O2, O1W—H2W…O4 and O3—H3O…O1W hydrogen bond (Table 4 and Fig. 2a). In addition, molecules are connected through C—H···O hydrogen bonds, forming chains running along the b axis. (Fig.2b). In the crystal, intermolecular O—H…O and C—H…O hydrogen bonds involving the hydroxyl groups lead to the formation of three-dimensional framework (Fig. 3)**.** The crystal structure does not exhibit X—H···π-ring or π—π stacking interactions. The detailed parameters of hydrogen bonds are given in Table 3.

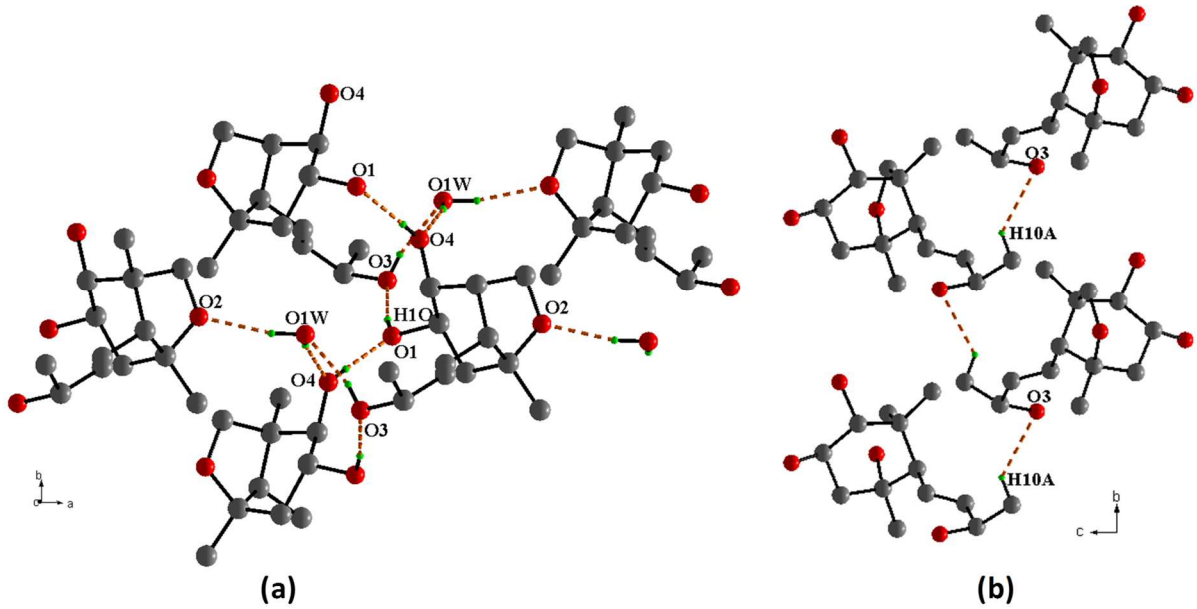

Figure 2 : A fragment of the title structure, showing molecules connected by (a) O–H···O and (b) C–H···O hydrogen bonds as dashed orange lines.

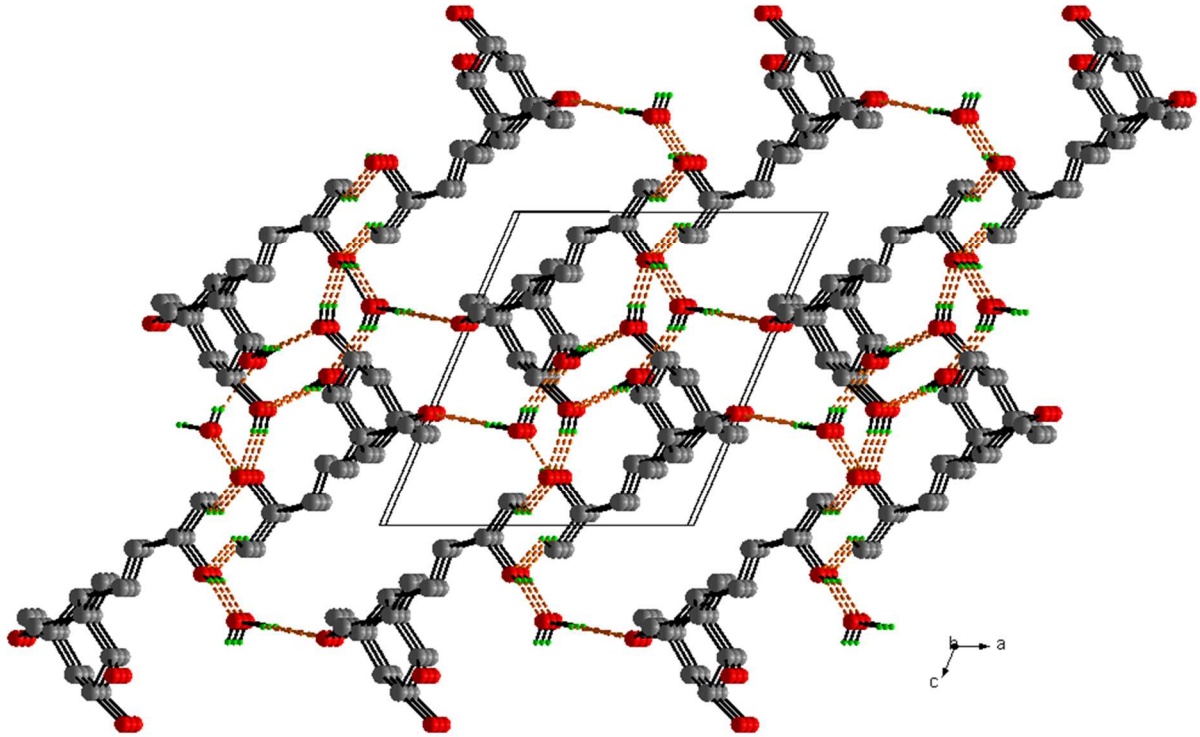

Figure 3 : Packing view showing the O–H···O and C–H···O hydrogen bonds as dashed lines. H atoms not involved in hydrogen bonding have been omitted for clarity.

Optimized molecular structure

The optimized molecular structure of (1S,2R,3R,5R,8R)-8-((R,E)-3-hydroxybut-1-en-1-yl)-1,5-dimethyl-6-oxabicyclo[3.2.1]octane-2,3-diol hydrate obtained by DFT and HF is shown in Fig. 1. Selected Geometric parameters from the X-ray analysis were compared with the theoretical values of optimized structure are presented in Table 3. The bond lengths calculated by HF method are little shorter than those by DFT/B3LYP method. We notice some small differences between some values such as for example C1—C6 and C5—C6, in the bicyclic ring, bonds lengths in crystal structure are 1.541(3) and 1.529(3) Å, whereas in DFT-optimized, the calculated values are 1.564 and 1.550 Å, respectively. The calculated values of C—H bond lengths of methyl part according to HF and B3LYP methods are also in good agreement. From the theoretical values, we found most of the optimized bond lengths are in a good agreement with experimental bond lengths but bond angles are slightly longer and shorter than that of experimental values. This sensitive gap is attributed to the difference between the solid phase and gas phase model.

Table 3: Experimental and calculated geometric parameters (Å, °) for compound $C_{13}H_{22}O_4.H_2O$

Bond	X-ray	DFT	HF	Bond	X-ray	DFT	HF
O1W—H1W	0.78 (4)	0.965	0.944	C6—C1	1.541(3)	1.564	1.549
O1W—H2W	0.83 (4)	0.979	0.950	C6—H6	0.98	1.098	1.087
O1—C3	1.426(3)	1.436	1.414	C1—C12	1.522(3)	1.528	1.526
O1—H1O	0.82 (3)	0.969	0.945	C1—C11	1.534(3)	1.538	1.533
O2—C11	1.441(3)	1.435	1.412	C1—C2	1.542(3)	1.547	1.541
O2—C5	1.466(3)	1.449	1.423	C2—C3	1.529(3)	1.534	1.528
O3—C9	1.423(3)	1.417	1.398	C2—H2	0.98	1.097	1.087
O3—H3O	0.78(4)	0.974	0.947	C3—C4	1.530(3)	1.531	1.526
O4—C2	1.426(3)	1.436	1.413	C3—H3	0.98	1.097	1.084
O4—H4O	0.86(3)	0.965	0.942	C4—C5	1.524(3)	1.544	1.535
C10—C9	1.509(3)	1.538	1.529	C4—H4A	0.97	1.094	1.083
C10—H10A	0.96	1.096	1.087	C4—H4B	0.97	1.094	1.084
C10—H10B	0.96	1.096	1.087	C5—C13	1.513(3)	1.522	1.518
C10—H10C	0.96	1.093	1.084	C11—H11A	0.97	1.097	1.084
C9—C8	1.500(3)	1.515	1.513	C11—H11B	0.97	1.099	1.087
C9—H9	0.98	1.091	1.087	C13—H13A	0.96	1.094	1.084
C8—C7	1.318(3)	1.335	1.319	C13—H13B	0.96	1.094	1.084
C8—H8	0.93	1.085	1.081	C13—H13C	0.96	1.094	1.084
C7—C6	1.503(3)	1.502	1.504	C12—H12A	0.96	1.095	1.086
C7—H7	0.93	1.085	1.072	C12—H12B	0.96	1.095	1.086
C6—C5	1.529(3)	1.550	1.541	C12—H12C	0.96	1.095	1.086
Angles							
H1W—O1W—H2W	102 (3)	104.8	106.4	C3—C2—H2	108.8	108.4	108.5
C3—O1—H1*O*	111.0(2)	105.4	107.9	C1—C2—H2	108.8	108.0	108.3
C11—O2—C5	109.0(2)	109.7	110.8	O1—C3—C2	110.5(2)	109.5	109.7
C9—O3—H3*O*	106 (2)	109.8	111.1	O1—C3—C4	108.4(2)	108.8	108.7
C2—O4—H4*O*	108 (2)	108.2	110.3	C2—C3—C4	113.5(2)	114.5	114.2
C9—C10—H10A	109.5	110.3	110.5	O1—C3—H3	108.1	108.6	108.8
C9—C10—H10B	109.5	111.5	111.3	C2—C3—H3	108.1	106.7	106.9
H10A—C10—H10B	109.5	108.0	108.0	C4—C3—H3	108.1	108.5	108.4
C9—C10—H10C	109.5	109.8	109.9	C5—C4—C3	112.0(2)	111.0	110.9
H10A—C10—H10C	109.5	109.8	108.4	C5—C4—H4A	109.2	110.8	110.9
H10B—C10—H10C	109.5	108.6	108.6	C3—C4—H4A	109.2	109.8	110.0
O3—C9—C8	112.2(2)	113.5	113.3	C5—C4—H4B	109.2	109.3	109.3
O3—C9—C10	111.0(2)	111.4	111.1	C3—C4—H4B	109.2	109.0	108.6
C8—C9—C10	112.6(2)	110.9	111.0	H4A—C4—H4B	107.9	106.8	106.9
O3—C9—H9	106.9	104.8	105.1	O2—C5—C13	108.1(2)	108.0	108.4
C8—C9—H9	106.9	108.1	107.9	O2—C5—C4	108.3(2)	107.9	107.8
C10—C9—H9	106.9	107.7	108.1	C13—C5—C4	112.2(2)	112.0	112.0
C7—C8—C9	126.2(2)	123.4	124.4	O2—C5—C6	102.3(2)	103.4	102.9
C7—C8—H8	116.9	120.7	120.3	C13—C5—C6	114.8 (2)	114.4	114.4
C9—C8—H8	116.9	115.9	115.3	C4—C5—C6	110.5(2)	110.5	110.8
C8—C7—C6	123.7(2)	126.2	125.2	O2—C11—C1	106.6(2)	106.7	106.7
C8—C7—H7	118.2	116.4	117.3	O2—C11—H11A	110.4	109.6	109.8
C6—C7—H7	118.2	117.3	117.4	C1—C11—H11A	110.4	112.2	112.8
C7—C6—C5	116.2(2)	116.2	116.3	O2—C11—H11B	110.4	109.2	109.2
C7—C6—C1	116.8(2)	115.9	116.9	C1—C11—H11B	110.4	110.8	110.8
C5—C6—C1	100.4(2)	99.2	99.2	H11A—C11—H11B	108.6	108.0	108.1
C7—C6—H6	107.6	109.5	108.8	C5—C13—H13A	109.5	110.5	110.3
C5—C6—H6	107.6	108.0	107.6	C5—C13—H13B	109.5	110.7	110.8
C1—C6—H6	107.6	107.2	107.3	H13A—C13—H13B	109.5	108.5	108.6
C12—C1—C11	113.8(2)	113.2	112.8	C5—C13—H13C	109.5	110.2	110.3
C12—C1—C6	113.3(2)	113.9	114.0	H13A—C13—H13C	109.5	108.2	108.2
C11—C1—C6	99.4(2)	99.7	99.1	H13B—C13—H13C	109.5	108.6	108.7
C12—C1—C2	110.6(2)	111.1	111.2	C1—C12—H12A	109.5	110.9	110.7
C11—C1—C2	109.9(2)	111.0	110.9	C1—C12—H12B	109.5	111.0	111.2
C6—C1—C2	109.2(2)	107.4	108.1	H12A—C12—H12B	109.5	107.7	108.6
O4—C2—C3	106.6(2)	104.3	104.9	C1—C12—H12C	109.5	111.3	111.3
O4—C2—C1	111.2(2)	113.7	113.1	H12A—C12—H12C	109.5	107.4	107.4
C3—C2—C1	112.7(2)	113.0	112.8	H12B—C12—H12C	109.5	108.5	107.6
O4—C2—H2	108.8	109.3	109.0				

Table 4
Hydrogen-bond geometry (Å, º) for $C_{13}H_{22}O_4.H_2O$

D*—H···*A	***D*—H**	**H···*A***	***D*···*A***	***D*—H···*A***
O1*W*—H1*W*···O2^{i}	0.78 (4)	2.09 (4)	2.867 (3)	173 (4)
O3—H3*O*···O1*W*	0.78 (4)	1.98 (4)	2.718 (3)	157 (3)
O1*W*—H2*W*···O4^{ii}	0.83 (4)	1.96 (4)	2.776 (3)	167 (3)
O4—H4*O*···O1^{iii}	0.86 (3)	1.82 (3)	2.674 (2)	174 (3)
C10—H10*A*···O3^{iv}	0.96	2.51	3.264 (4)	135
O1—H1*O*···O3^{iii}	0.82 (3)	1.87 (3)	2.685 (3)	172 (3)
C7—H7···O3	0.96	2.49	2.829(4)	102

Symmetry codes: (i) *x*-1, *y*, *z*; (ii) -*x*+1, *y*-1/2, -*z*+1; (iii) -*x*+1, *y*+1/2, -*z*+1; (iv) -*x*+1, *y*+1/2, -*z*+2.

3.3. Hirshfeld surface analysis

For specifying the diverse intermolecular interactions in $C_{13}H_{22}O_4.H_2O$ compound, the d_{norm}, and 2D finger print plots are depicted in Fig. 4 and 5 respectively. The red spots on the Hirshfeld surface represent O—H…O contacts while the blue regions correspond to weak interactions such as C—H…O contacts. The overall two-dimensional fingerprint plot, Fig. 5a, and those delineated into H…H, H…O/O…H and H…C/C…H contacts are illustrated in Fig. 5 b–c, respectively, together with their relative contributions to the Hirshfeld surface. The H…H interactions (75.2%) are the major factor in the crystal packing, which is reflected in Fig. 5b as widely scattered points of high density due to the large hydrogen content of the molecule with the small split tips at $d_e \approx d_i \approx 1.1$ Å.

The O…H/H…O interactions (24.6%) representing the next highest contribution (Fig. 5c). between the oxygen atoms inside the surface and the hydrogen atoms outside the surface and vice versa, $d_e + d_i \approx 1.75$ Å are shown two symmetrical points at the top, bottom left and right, which are characteristic of O—H···O hydrogen bond and contact such as C…H/H…C (0.2%) make a small contribution to the entire Hirshfeld surface.

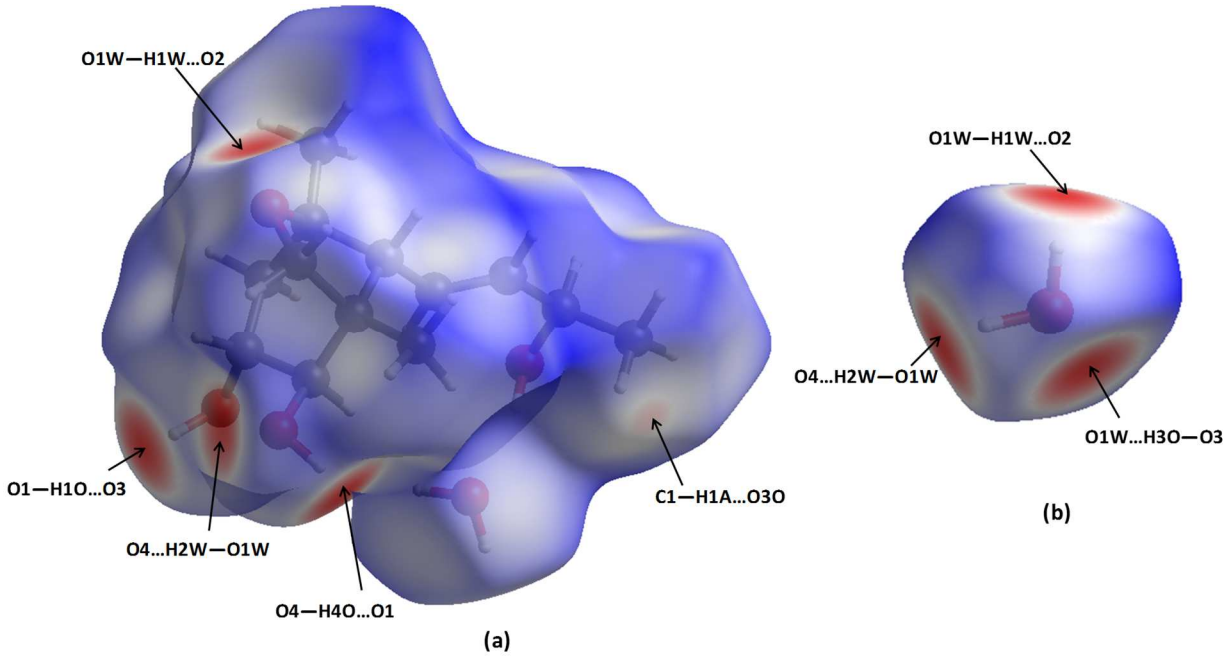

Figure 4 : Views of the three-dimensional Hirshfeld surface for the title compound plotted over d_{norm} (a) *Euphorbioside* and (b) water molecule.

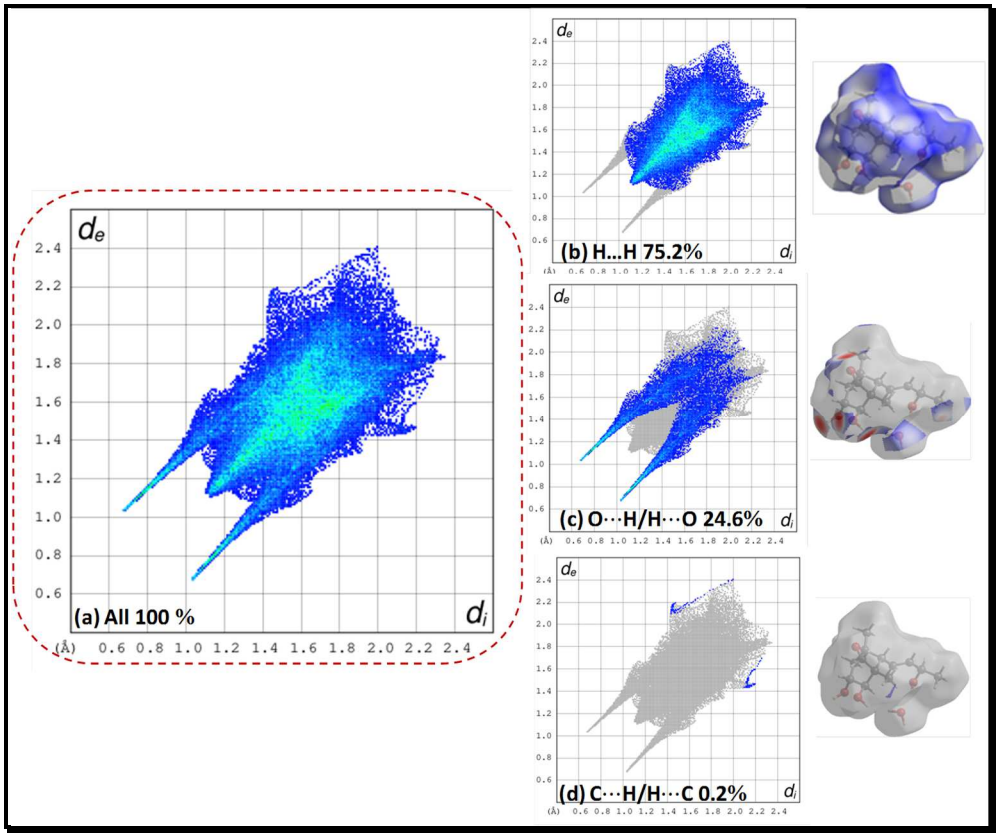

Figure 5: Two-dimensional fingerprint plots and relative contributions of various interactions to the Hirshfeld surface of the title compound corresponding to (a) all interactions, (b) H···H, (c) H···O/O···H and (d) C···H/H···C.

3.4 Frontier Molecular Orbitals (FMOs)

The DFT calculations provide some important information on the reactivity and site selectivity of the molecular framework. The energy of the HOMO is directly related to the ionization potential, while the energy of LUMO is related to electron affinity and the energy gap between the HOMO and LUMO characterizes the molecular chemical stability. The energy levels of the HOMO and LUMO for compound are illustrated in Fig. 6. Red and green color distributions represent positive and negative phase in molecular orbital wave function, respectively. The electron density of HOMO and LUMO in the title compound is concentrated in the plane of the whole (-3-hydroxybut-1-en-1-yl)-6-oxabicyclo[3.2.1]octane-2,3-diol. The energies of HOMO and LUMO, energy gap, electronegativity (χ), chemical hardness (η), global softness (ξ) and electrophilicity (ψ) index are calculated and presented in Table 5. The calculated chemical hardness, softness and chemical potential values for the studied molecule were found to be 3.044eV, 0.164eV^{-1} and 3.442eV, respectively. The energy gap of the molecule is calculated about 6.089eV. This large HOMO-LUMO gap is an indication of a good stability and a high chemical hardness for the title compound.

Table 5: HOMO–LUMO energies and values of quantum chemical parameters calculated by B3LYP/6-31G (d,p)

	6-31g(d,p)	**HF-6-31g(d,p)**
E_T (eV)	-24098.143	-23952.054
E_{HOMO} (eV)	-6.487	-9.424
E_{LUMO} (eV)	-0.398	4.709
$\Delta E_{(LUMO-HOMO)}$ (eV)	**6.089**	**14.133**
Global hardness (η)	3.044	7.066
Softness (ξ)	0.164	0.071
Chemical potential (μ)	3.442	2.357
Electrophilicity (ψ)	1.943	0.395
Electronegativity (χ)	-3.442	-2.357
Dipole moment (D)	2.114	2.194

$\eta=1/2[E_{LUMO}-E_{HOMO}]$, $\xi=1/2\eta$, $\mu= -[1/2(E_{LUMO}+E_{HOMO})]$, $\psi= \mu^2/2\eta$, $\chi = -\mu$

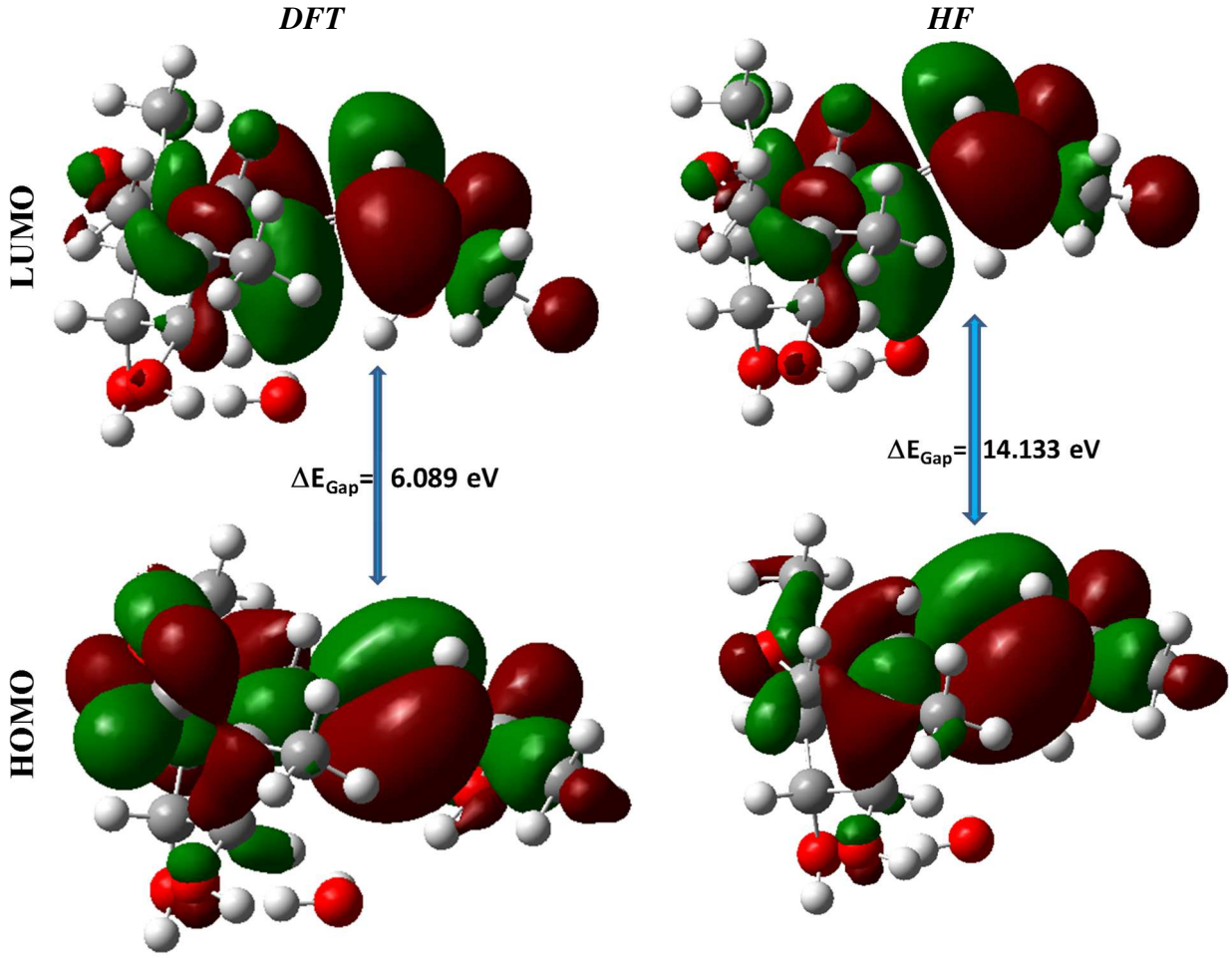

Figure 6: 3D plots of frontier molecular orbital of $C_{13}H_{22}O_4.H_2O$ obtained by DFT and HF methods.

3.4 Molecular Properties

3.4.1 Atomic charges

The Mulliken charge values were calculated using B3LYP and HF functionals with 6-31G(d,p) basis set for the $C_{13}H_{22}O_4.H_2O$ structure. In Table 6, Mulliken charges and natural atomic charges for all atoms in the molecule (1S,2R,3R,5R,8R)-8-((R,E)-3-hydroxybut-1-en-1-yl)-1,5-dimethyl-6-oxabicyclo[3.2.1]octane-2,3-diol hydrate are reported. The C2/C3/C5/C9 atoms of the molecule exhibit positive charge while the other carbon has negative charges in Mulliken and natural atomic charges except the charge of atom C11 is positive in Mulliken, while in NBO this charge is negative.. The charge distribution showed that carbon atoms attached to electronegative atoms (Oxygen) have positive charges. Moreover, all the hydrogen atoms attached to water molecule and O1, O3 and O4 atoms have a net positive charge. This result reveals that there is charge transfer through the O—H···O

hydrogen bonds. It should be noted that in the presence of the water molecule the charges of the oxygen atoms are not affected except for the O3 atom as it evident from O3 (-0.537e) (Fig. SI7) and presence of intermolecular hydrogen bonding the same atom shows that O3 (-0.571e)

Table 6: Mulliken and natural atomic charge of $C_{13}H_{22}O_4.H_2O$ compound by DFT and HF methods

	Mulliken		**NBO**	
	DFT	***HF***	***DFT***	***HF***
O1W	-0.642	-0.716	-0.993	-1.003
H1W	0.314	0.343	0.485	0.485
H2W	0.331	0.374	0.503	0.514
O1	-0.569	-0.690	-0.779	-0.823
H1*O*	0.323	0.354	0.499	0.501
O2	-0.546	-0.690	-0.599	-0.663
O3	-0.571	-0.675	-0.777	-0.812
H3*O*	0.321	0.358	0.496	0.502
O4	-0.569	-0.680	-0.776	-0.816
H4*O*	0.314	0.345	0.489	0.491
C1	-0.008	-0.146	-0.102	-0.106
C2	0.127	0.203	0.066	0.091
H2	0.102	0.133	0.233	0.232
C3	0.163	0.219	0.080	0.109
H3	0.118	0.143	0.239	0.239
C4	-0.184	-0.217	-0.509	-0.492
H4A	0.111	0.140	0.258	0.258
H4B	0.101	0.124	0.245	0.241
C5	0.277	0.285	0.300	0.319
C6	-0.118	-0.170	-0.297	-0.294
H6	0.088	0.136	0.258	0.254
C7	-0.053	-0.116	-0.255	-0.249
H7	0.085	0.158	0.234	0.242
C8	-0.109	-0.179	-0.230	-0.230
H8	0.074	0.127	0.223	0.224
C9	0.159	0.224	0.078	0.105
H9	0.102	0.128	0.235	0.237
C10	-0.321	-0.342	-0.706	-0.698
H10A	0.094	0.105	0.230	0.228
H10B	0.116	0.131	0.244	0.244
H10C	0.100	0.108	0.227	0.224
C11	0.092	0.158	-0.109	-0.077
H11A	0.085	0.108	0.215	0.214
H11B	0.105	0.132	0.227	0.231
C12	-0.345	-0.331	-0.690	-0.678
H12A	0.107	0.124	0.244	0.241
H12B	0.111	0.121	0.242	0.238
H12C	0.102	0.117	0.236	0.235
C13	-0.316	-0.303	-0.693	-0.674
H13A	0.112	0.125	0.244	0.243
H13B	0.108	0.120	0.243	0.239
H13C	0.109	0.118	0.243	0.236

3.4.2 Molecular Electrostatic Potentiel (MEP)

Molecular electrostatic potential map gives information about the electron rich and electron deficient parts of the investigated molecule. In order to study the site of $C_{13}H_{22}O_4.H_2O$ available for electrophilic and nuclephilic attack, the MEP is plot of electrostatic potential mapped onto the constant electron density surface. Molecular electrostatic potential of $C_{13}H_{22}O_4.H_2O$ using B3LYP/6-311G (d, p) optimized geometry is computed, contour and surface map is shown in Fig. 7. The negative electrostatic potential is indicated by red regions, the blue region indicates the positive electrostatic potential, the yellow region reveals the slightly rich electron and the green region shows neutral potential. The electrostatic potential of the title compound is in the range $-5.935x10^{-2}$ V to $5.935x10^{-2}$ V. The total electron density surface mapped with electrostatic potential indicates the presence of a high negative potential region around oxygen atoms. While the positive region of the MEP map is localized over the H-hydroxyl and H-water group, indicating that they are susceptible sites for nucleophilic attack.

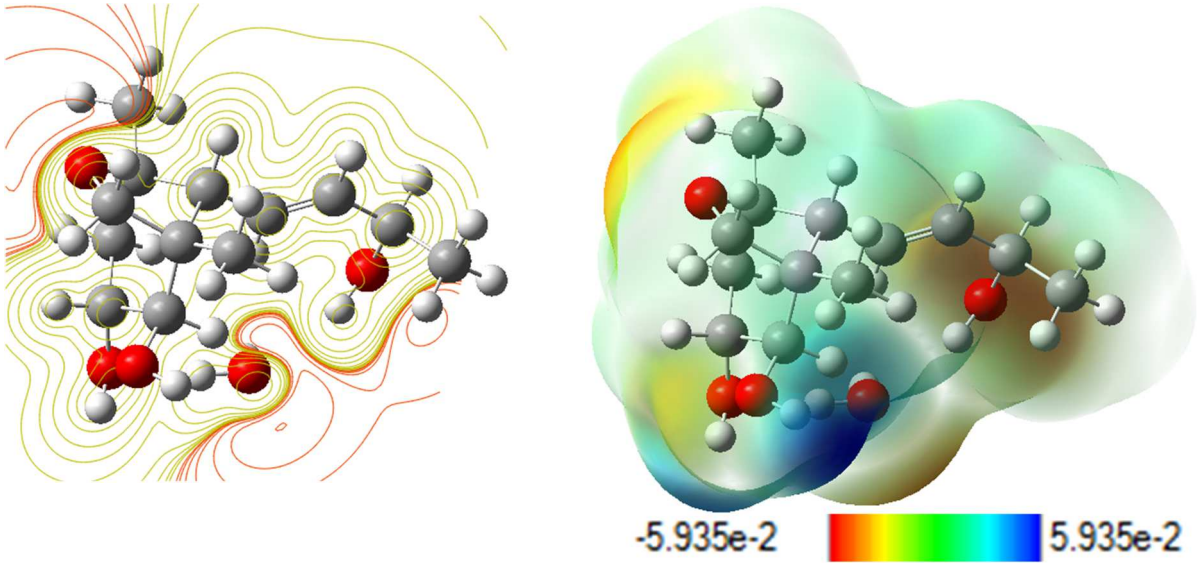

Figure 7: (a) the contour map of electrostatic potential and (b) the total electron density mapped with electrostatic potential of $C_{13}H_{22}O_4.H_2O$ at an isosurface value of 0.020 a.u. and an isodensity of 0.0004 a.u.

3.4.3 Nonlinear Optical Properties (NLO)

The polarizabilty, first polarizability and dipole moment is calculated using B3LYP/6-31g(d,p) basis set and can be obtained by a frequency job output file of Gaussian. The complete equations for calculating the mean dipole moment, polarizability and the first hyperpolarizability are as follows:

$$\mu_{tot} = (\mu_x^2 + \mu_y^2 + \mu_z^2)^{1/2}$$

$$\alpha_{tot} = \frac{1}{3}(\alpha_{xx} + \alpha_{yy} + \alpha_{zz})$$

$$\beta = [(\beta_{xxx} + \beta_{xyy} + \beta_{xzz})^2 + (\beta_{yyy} + \beta_{yzz} + \beta_{yxx})^2 (\beta_{zzz} + \beta_{zxx} + \beta_{zyy})^2]^{1/2}$$

The values of dipole moment, polarizability and the first hyperpolarizability for the title compound are reported in Table 7. The polarizabilities and hyperpolarizability are reported in atomic units (a.u), converted into electrostatic units (esu) (α: 1a.u = 0.1482 x 10^{-24} esu, β: 1a.u. = 8.6393x10^{-33}esu). The result shows total molecular dipole moment was found to be 2.114 D. The highest value of dipole moment is observed for component μ_z (2.0355D). The calculated first order hypolarizability for Eurobioside hydrate molecule is equal to 0.5322 10^{-30} esu.

Table 7: The calculated dipole moment μ (D), polarizability α (x 10^{-24}esu) and the first hyperpolarizabiliyu β (x 10^{-33}esu) of *Eurobioside* hydrate obtained by B3LYP level with the 6-31g(d,p) basis sets.

	a.u	**esu (x10^{-24})**		**a.u**	**esu (x10^{-33})**
μ_x	0.4581		β_{xxx}	2.9582	51.3339
μ_y	-0.3386		β_{xxy}	1.2915	6.8898
μ_z	2.0355		β_{xyy}	-0.6441	4.7231
μ_{total} **(D)**	2.114		β_{yyy}	33.9454	315.2691
α_{xx}	-122.2619	-18.0888	β_{xxz}	14.4666	131.1939
α_{xy}	6.1174	0.9995	β_{xyz}	1.2614	4.4225
α_{yy}	-107.3340	-15.8097	β_{yyz}	3.0386	20.6575
α_{xz}	-1.4077	-0.10488	β_{xzz}	5.1663	48.7888
α_{yz}	-0.8483	-0.1556	β_{yzz}	21.4895	194.5762
α_{zz}	-102.9594	-15.2359	β_{zzz}	5.3104	60.0916
α_{total}	-110.8518	-16.4282	β	61.5986	532.1691

3.4.4 Natural bond orbital (NBO) analysis

The natural population analysis performed on the electronic structure of the title molecule clearly explains the distribution of electron in various subshells of their atomic orbital. The natural bond orbital study of the title molecule was computed at B3LYP and HF with 6-31g(d,p) level of model. Tables SI1-2 regroup the electron in the core, valence and Rydberg sub shells of the the molecule. The most electronegative atoms O1w, O1, O3 and O4 have charges -0.99326, -0.77910, -0.77683 and -0.77621 respectively. While the most electropositive atom is C5 with charge 0.29997 (Table SI1). The natural population analysis show that the distribution of 142 electrons in the title compound. The structure of the calculated compound was exhibited a type of Lewis structure (99.15%), 0.68% of valence non-Lewis and 0.16% of Rydberg non Lewis (Fig.8 and Table SI3).

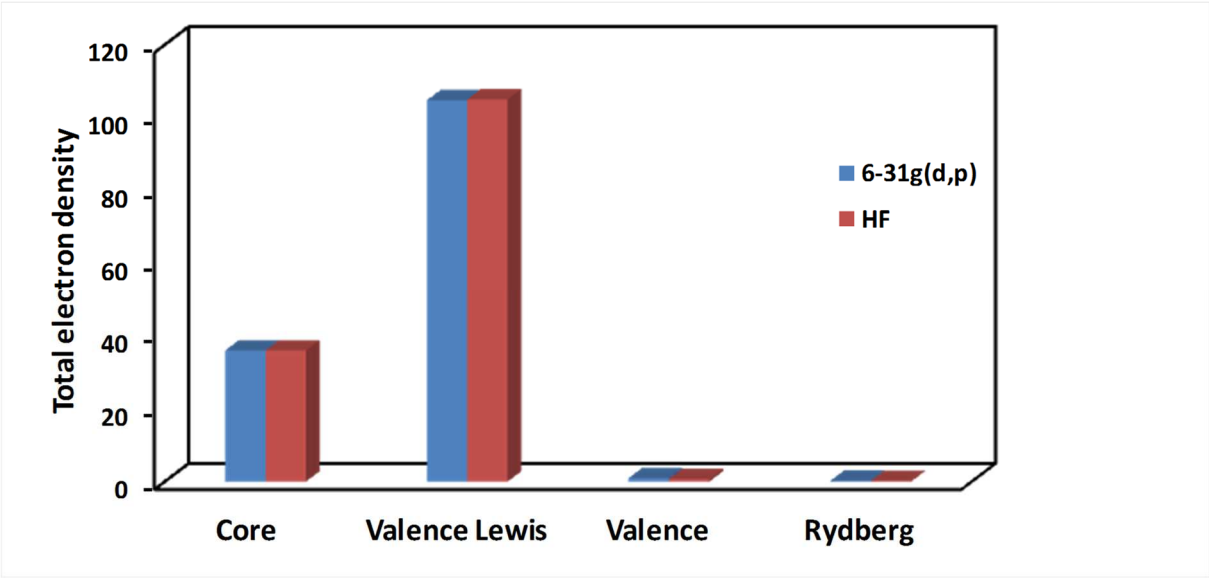

Figure 8 : Percentage contribution of natural population analysis and natural Lewis structure of the title compound.

Natural bond orbital (NBO) analysis has been performed to elucidate the intramolecular and the interaction which will weaken the bond associated with the anti-bonding orbital in a molecule. For each donor NBO (*i*) and acceptor NBO (*j*), the stabilization energy $E^{(2)}$ associated with delocalization *i* -> *j* is estimated as :

$$E^{(2)} = \Delta E_{ij} = q_i \frac{F(i,j)^2}{E_j - E_i}$$

q_i : donor orbital occupancy,
E_i, E_j diagonal elements,
F_{ij} the off diagonal NBO Fock matrix element.

The larger $E^{(2)}$ values representing the more intensive in the interaction between electron donors and electron acceptors. NBO analysis has been performed on the title compound at B3LYP/6-31g(d,p) method and results are summarized in Table 8. The NBO analysis of the title compound can clearly explain the evidence of the formation of H – bonded interaction between the LP(O) and σ(O-H) antibonding orbitals. The stabilization energy $E^{(2)}$ associated with hyperconjucate interaction LP(1)O1→ σ*(O1w-H2w), LP(2)O1→ σ*(O1w-H2w) and LP(2)O1w→ σ*(O3-H3*O)* with 1.46, 13.15 and 7.39 Kcal/mol.

Table 8: Second Order Perturbation Theory Analysis of Fock Matrix in NBO Basis calculated at B3LYP/6-31g(d,p) level

Donor (i)	**ED(i)/e**	**Acceptor (j)**	**ED (j)/e**	**E(2)[a] Kcal/mol**	**E(j)-E(i)[b] a.u**	**F(i.j)[c] a.u**
From unit 1 to unit 2						
LP(1)O1w	1.99279	σ*(O3-H3*O)*	0.02562	0.80	0.96	0.025
LP(2)O1w	1.97109	σ*(O3-H3*O)*	0.02562	7.39	0.90	0.073
		σ*(C7-H7)	0.03074	1.30	0.91	0.031
From unit 2 to unit 1						
LP(1)O1	1.97530	σ*(O1w-H2w)	0.03577	1.46	1.02	0.035
LP(2)O1	1.93963	σ*(O1w-H2w)	0.03577	13.15	0.86	0.096
Within unit 2						
LP(1)O1	1.97530	σ*(C2–C3)	0.03960	3.72	0.92	0.052
LP(2)O1	1.93963	σ*(C3-H3)	0.02737	5.51	0.84	0.061
LP(1)O2	1.96839	σ*(C1-C6)	0.04203	2.46	0.91	0.042
		σ*(C1-C11)	0.03188	3.05	0.92	0.047
LP(2)O2	1.92629	σ*(C4-C5)	0.03835	7.09	0.65	0.061
		σ*(C11-H11B)	0.02364	5.62	0.73	0.058
LP (1)O3	1.97729	σ*(C10-C9)	0.03074	1.24	0.93	0.031
		σ*(C9-C8)	0.03662	2.19	0.98	0.041
LP (2)O3	1.94862	σ*(C10-C9)	0.03074	7.22	0.65	0.061
		σ*(C9-C8)	0.03662	6.07	0.70	0.058
LP(1)O4	1.98109	σ *(C2-H2)	0.02823	2.47	1.05	0.045
LP(2)O4	1.95231	σ*(C1–C2)	0.04950	8.33	0.68	0.067
		σ *(C2-H2)	0.02823	2.23	0.77	0.037

[a] $E^{(2)}$ means energy of hyper conjugative interaction (stabilization energy)
[b] Energy difference between donor and acceptor i and j NBO orbitals
[c] F(i, j) is the Fork matrix element between i and j NBO orbitals

Conclusion

(1S,2R,3R,5R,8R)-8-((R,E)-3-hydroxybut-1-en-1-yl)-1,5-dimethyl-6 oxabicyclo[3.2.1]octane-2,3-diol hydrate has been isolated from latex of *Euphorbia resinifera* Berg and its crystal structure has been characterised by single-crystal X-ray diffraction and different spectroscopic techniques (IR, LC/HRMS, and NMR). X-ray crystallographic studies for the title compound display intermolecular O—H···O and O—H···O hydrogen bonding forming three-dimensional framework. Hirshfeld surface analysis determining the diverse intermolecular interactions in $C_{13}H_{22}O_4.H_2O$ molecule provides the hydrogen-bond donor and hydrogen-bond acceptor areas. MEP map gives information about the negative sites being intensified mostly over O atoms. This large HOMO-LUMO gap is an indication of a good stability and a high chemical hardness for the title compound. The stabilization of the structure has been identified by second order perturbation energy calculations.

Acknowledgments

The authors are greatly thankful to the Campus France (PHC Toubkal 17/55 Campus France 36758 VA), National Centre for Scientific and Technical Research (CNRST) of Morocco for its support, Dr. Laurenr Jouffret (UCA-PARTNER, Institut de Chimie de Clermont-Ferrand, CNRS, Université Clermont Auvergne, SIGMA Clermont, Clermont-Ferrand, France) for the X-ray measurements and Dr. Salha Hamri (Assistant Professor; Laboratory of Organic Chemistry, Organometallic and Valorization of Natural Substances, Faculty of Sciences, Ibn Zohr University, Agadir-Morocco) for latex collect..

References

[1] A. Fournet, V. Muñoz, Natural products as trypanocidal, antileishmanial and antimalarial drugs. *Curr. Top. Med. Chem.*, *2* (2002), 1215 – 1237.

[2] D. J. Newman, G. M. Cragg, Natural products as sources of new drugs over the last 25 years. *J. Nat. Prod.*, 70 (2007), 461 – 477.

[3] A. Singla, K. Pathak, Phytoconstituents of Euphorbia species*, Fitoterapia.*, *41* (1990), 483-516.

[4] H. Q. Chen, H. Wang, B. Yang, D. Q. Jin, S. L. Yang, M. C. Wang, J. Xu, Y. Ohizumi, Y. Q. Guo, Diterpenes inhibiting NO production from *Euphorbia helioscopia*. Fitoterapia., 95 (2014), 133-135.

[5] C. Y. Ragasa, K. B. Cornelio, Triterpenes from Euphorbia hirta and their cytotoxicity. *J. Nat. Med*., 11 (2013), 528–533.

[6] X. Y. Wang, L. P. Liu, T. G. Kang, H. B. Wang, Chemical constituents of Euphorbia fischeriana. *J. Nat. Med*., 10 (2012), 299–302.

[7] G. Appendino, P. Spagliardi, M. Ballero, G. Seu, Macrocyclic diterpenoids from *Euphorbia hyberna* L. subsp. *insularis* and their reaction with oxyphilic reagents. *Fitoterapia*., 73 (2002), 576–582.

[8] S. Wang, H. Liang, Y. Zhao, G. Wang, H. Yao, R. Kasimu, Z. Wu, Y. Li, J. Huang, J. Wang, New triterpenoids from the latex of *Euphorbia resinifera* Berg. *Fitoterapia*., 108 (2016), 33–40.

[9] E. Fattorusso, V. Lanzotti, O. Taglialatela-Scafati, G. C. Tron, G. Appendino, Bisnorsesquiterpenoids from *Euphorbia resinifera* Berg. and an Expeditious Procedure to Obtain Resiniferatoxin from Its Fresh Latex. *Eur. J. Org. Chem.,* (2002), 71-78.

[10] P. A. Wender, C. D. Jesudason, H. Nakahira, N. Tamura, A. L. Tebbe, Y. J. Ueno, The First Synthesis of a Daphnane Diterpene: The Enantiocontrolled Total Synthesis of (+)-Resiniferatoxin". *Am. Chem. Soc*., 119 (1997), 12976−12977.

[11] S. Hashimoto, S.-I. Katoh, T. Kato, D. Urabe, M. Inoue, Total Synthesis of Resiniferatoxin Enabled by Radical-Mediated Three-Component Coupling and 7-endo Cyclization. *J. Am. Chem. Soc*., 139 (2017), 16420-16529.

[12] T. K. Allred, F. Manoni, P. G. Harran, Exploring the Boundaries of "Practical": De Novo Syntheses of Complex Natural Product-Based Drug Candidates. *Chem. Rev*., 117 (2017), 11994-12051.

[13] G. Appendino, A. Szallasi, Euphorbium: Modern research on its active principle, resiniferatoxin, revives an ancient medicine. *Life Science*., 60 (1997), 681-696.

[14] Bruker (2016). *APEX3* (Version 5.054), *SAINT+* (Version 6.36A), *SADABS*. Bruker AXS Inc., Madison, Wisconsin, USA.

[15] G. M. Sheldrick, SHELXT - Integrated space-group and crystal-structure determination. *Acta Crystallogr. Sect. A Found*. Crystallogr., 71 (2015), 3–8.

[16] G. M. Sheldrick, Crystal structure refinement with SHELXL. *Acta Crystallogr. Sect. C Struct. Chem*., 71 (2015), 3–8.

[17] K. Brandenburg . *DIAMOND*. Crystal Impact GbR, B *Bonn, Germany* (2006).

[18] M. A. Spackman, D. Jayatilaka, Hirshfeld surface analysis. *CrystEngComm*., 11 (2009), 19–32.

[19] J. J. McKinnon, D. Jayatilaka, M. A. Spackman, Towards quantitative analysis of intermolecular interactions with Hirshfeld surfaces. *Chem. Commun*., (2007), 3814–3816.

[20] M. J. Turner, J. J. MacKinnon, S. K. Wolff, D. J. Grimwood, P. R. Spackman, D. Jayatilaka, M. A. Spackman, *Crystal Explorer 17.5*. University of Western Australia, Perth, Australia. (2017).

[21] M. Frisch, G. Trucks, H. Schlegel, G. Scuseria, Gaussian 09, revision D. 01, (2009).

[22] A. Frisch, A. Nielson, A. J. Holder, Gaussview user manual. *Gaussian Inc., Pittsburgh, PA*, 556 (2000).

[22] A. D. Becke, Density-functional thermochemistry. The role of exact exchange. *J. Chem. Phys*., 98 (1993), 5648–5652.

[24] C. Lee, W. Yang, R. G. Parr, Development of the Colle-Salvetti correlation-energy formula into a functional of the electron density. *Phys. Rev B*., 37 (1988), 785-789.

[25] G. Miehlich, A. Savin, A. Stoll, H. Preuss, Results obtained with the correlation energy density functionals of becke and Lee, Yang and Parr. *Chemical Physics Letters*., 157 (1989), 200-206.

[26] E. D. Glendening, J. K. Badenhoop, A. E. Reed, J. E. Carpenter, J. A. Bohmann, C. M. Morales, F. Weinhold, NBO 5.0, Theoretical Chemistry Institute, University of Wisconsin, Madison, (2001).

[27] J.-G. Shi, Y.-P. Shi, Z.-J. Jia, Sesquiterpenoids from *Euphorbia wangii. Phytochemistry*., *45* (1997), 343-347.

[28] H. Farah, A. Ech-chahad, A. Lamiri, Semi-synthesis and Antimicrobial activities of some new Euphorbioside derivatives. *Int. J. Chem Tech. Res*., 6 (2014), 763-767.

[29] M. A. Lloyd, G. E. Patterson, G. H. Simpson, L. L. Duncan, D. P. King, Y. Fu, B. O. Patrick, S. Parkin, C. P. Brock, Solid-state compounds of stereoisomers: cis and trans isomers of 1,2-cyclohexanediol and 2,3-tetralindiol. *Acta Cryst*. B63 (2007) 433-447.

[30] R. Outouch, S. Oubaassine, M. Ait Ali, L. El Firdoussi, A. Spannenberg, Crystal structure of (1S,2R,4S)-1-[(morpholin-4-yl)- methyl]-4-(prop-1-en-2-yl)cyclohexane-1,2-diol. *Acta Cryst*. E71 (2015) 79–81.

[31] Y-S. Shi, L. Li, Y-B. Liu, S-G. Ma, Y. Li, J. Qu, Q. Liu, Z-F. Shen, X-G. Chen, S-S. Yu, A new thiophene and two new monoterpenoids from Xanthium sibiricum. *Journal of Asian Natural Products Research*. 17 (2015) 1039-1047.